EVALUATION OF SENSORS FOR A SMART WHEELCHAIR

Edmund F. LoPresti[1], Richard C. Simpson[1], David Miller[2], and Illah Nourbakhsh[3]
[1]AT Sciences, Pittsburgh, PA 15217, [2]Kiss Institute for Practical Robotics, Norman, OK 73072,
[3]Carnegie Mellon University, Pittsburgh, PA 15213

ABSTRACT

Seven sensors were evaluated to determine their ability to detect obstacles at different distances and angles. The Polaroid 600 and 9000 sonar sensors and Sharp GP2D02 and GP2D12 infrared sensors were evaluated for eight materials and four obstacle widths. The Massa E152/40, Sonaswitch Mini-A, and Devantech SRF04 sonar sensors were evaluated for a single condition.

BACKGROUND

Some individuals find it difficult or impossible to operate a standard power wheelchair (1). To accommodate this population, several researchers have developed "smart wheelchairs" which can detect objects in the environment and assist with obstacle avoidance, path following, or tasks such as moving through doorways (2). A smart wheelchair will only be as effective as its sensors. Sensor varieties could include traditional sonar, wide-beam sonar, infrared, bump sensors, and computer vision. It is important to understand the performance of these sensors under different conditions, so that a smart wheelchair will be able to assist people in a variety of environments.

RESEARCH QUESTIONS

Research is being conducted to evaluate a variety of commercially available sonar and infrared sensors. Characteristics of interest include minimum and maximum distances at which the sensor can detect an obstacle and the field of view of the sensor. The goal of this research is to measure these characteristics for a variety of sensors, a variety of materials which a smart wheelchair may encounter, and a variety of obstacle sizes.

METHOD

A series of tests were performed on four sensors: the Polaroid 600 sonar transducer (Polaroid, Cambridge, MA); the Polaroid 9000 wide-beam sonar transducer; the Sharp GP2D02 digital output infrared sensor (Sharp Electronics, Mahwah, NJ), and the Sharp GP2D12 analog output infrared sensor. Polaroid sensors were used in conjunction with the Polaroid Ultrasound Developers' Kit.

The range of each sensor was evaluated for a number of materials (Table 1). The sensor was initially positioned one meter from the obstacle, then moved toward the obstacle until the sensor no longer provided an accurate reading. The distance between the sensor and the obstacle was recorded as the minimum detection distance. The sensor was then moved away from the wall until the sensor no longer provided an accurate reading, and the distance between the sensor and the wall was recorded as the maximum detection distance. This test was repeated ten times for each sensor and each material condition.

The field of view of each sensor was evaluated for each material. Field of view was measured by the range of angles over which the sensor could detect a flat obstacle. Sonar sensors were placed 1 meter from the obstacle and infrared sensors were placed 8 cm from the obstacle. The angle between the sensor and the wall (in Figure 1) was varied starting from zero degrees (i.e. sensor perpendicular to the wall) and turning the sensor counterclockwise until the sensor no longer provided an accurate

Table 1: Materials tested and dimensions of obstacles.

Material	Width	Height	Depth
Bare drywall	48"	24"	0.5"
White drywall	48"	24"	0.5"
Black drywall	48"	24"	0.5"
Wood	48"	24"	0.25"
Glass	36"	12"	0.1"
Carpeting	60"	24"	32.5 oz face wt.
Marble	32"	9.5"	1"
Brick	15.5"	7"	3.75"

reading. The sensor was then turned clockwise until the sensor no longer provided an accurate reading. This procedure was repeated ten times for each obstacle.

Each sensor's detection angle was also measured using cardboard panels of varied width. Each panel was 2 meters long and 2 millimeters thick. Widths were 1.25 cm, 2.5 cm, 5.0 cm and 10.0 cm. The detection angle was measured as with the larger obstacles.

Preliminary evaluation was performed for three additional sensors. Minimum and maximum distance and field of view for the Massa E-152/40 (Massa Electronics, Hingham, MA) were measured for the bare drywall obstacle. Minimum and maximum distance and beam width were measured for the Sonaswitch Mini-A sensor (EDP Company, Livonia, MI) and the Devantech SRF04 (Robot Electronics, Norfolk, UK). Beam width was measured by moving targets toward the axis of the sensor (the horizontal line in Figure 1) from the left and the right side until the sensor detected the obstacle. Objects were moved into view until the sensor appeared to have at least a 50% probability of detecting the obstacle.

RESULTS

Minimum and maximum ranges of each sensor for each material condition are shown in Table 2. The Massa sensor had a minimum detection distance of 35.4 ± 2.1 cm and a maximum detection distance of 333.2 ± 24.8 cm for bare drywall. The Sonaswitch sensor had a minimum detection distance of 20.3 cm and a maximum distance of 99.1 cm. The Devantech sensor had a minimum detection distance of 2.5 cm and a maximum distance of 129.5 cm. Field of view (clockwise plus counterclockwise detection angles) are shown in Table 3 for each material condition, and in Table 4 for each size condition. The Polaroid 9000 was unable to detect the 1.25 cm wide obstacle, and the Polaroid 600 could only detect this obstacle 90% of the time. The Massa sensor had a total detection angle of $39.9^0 \pm 4.7^0$. The Sonaswitch sensor had beam widths of 21.6 cm at an obstacle distance of 0.3 m, and 27.9 cm at an obstacle distance of 0.61 m. The Devantech sensor had beam widths of 11.4 cm at an obstacle distance of 0.3 m, and 26.0 cm at an obstacle distance of 0.62 m.

Minimum detection distance for the GP2D12 was significantly lower than all other sensors ($p<0.05$ for Analysis of Variance using Fisher's Method). Minimum distance was significantly lower for GP2D02 than either ultrasound sensor ($p<0.05$), and for Polaroid 600 compared to Polaroid 9000 ($p<0.05$). Maximum distance was significantly higher for the ultrasound sensors compared to the infrared sensors, while detection angle was significantly higher for the infrared sensors compared to the ultrasound sensors ($p<0.05$). There were no significant material differences across sensors for detection range, although the minimum detection distance was significantly lower for carpeting compared to the majority of other materials for the Polaroid 600, GP2D02, and GP2D12. Differences in detection angle across materials may have been confounded by the different obstacle widths.

DISCUSSION

While the infrared sensors were able to detect closer obstacles and detect large obstacles at greater angles, the ultrasound sensors were able to detect obstacles at a larger distance. The Polaroid 9000 wide-beam sonar was able to detect small obstacles (2.5 to 10.0 cm) at a greater angle than the other sensors, but was unable to detect the 1.25 cm obstacle. The sensors also tended to react to materials in different ways. The GP2D12 in particular had difficulty detecting glass, black drywall, and black marble (significantly larger minimum and smaller maximum detection distances, $p<0.05$). The Sharp infrared sensors will be evaluated under

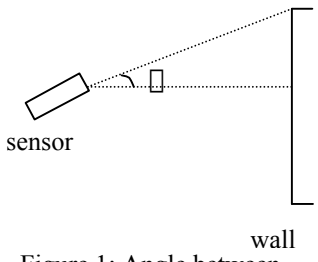

Figure 1: Angle between sensor and obstacle

different lighting conditions, since infrared detectors are sensitive to light. Further evaluation will also be performed for the Sonaswitch, Massa, and Devantech sensors.

Because of these differences between sensors, it would be beneficial to incorporate a variety of sensors into a smart wheelchair system. One limitation of this study is that all obstacles were stationary relative to the sensors. When incorporated in a smart wheelchair, the sensors will be moving relative to the obstacles, either because the sensors themselves are moving (on the wheelchair) or the obstacles are moving (e.g. people). Therefore, these results represent the best performance that can be expected for the sensors in real-world situations.

Table 2: Minimum and maximum detection distances across sensor models and obstacle materials. Values given as mean minimum ± standard deviation; mean maximum ± standard deviation. All measurements are in centimeters.

	Polaroid 600	Polaroid 9000	Sharp GP2D02	Sharp GP2D12
Bare drywall	8.1 ± 0.7; 275.7 ± 13.2	25.6 ± 0.6; 385.1 ± 16.1	3.0 ± 0.9; 56.8 ± 28.1	0.6 ± 0.1; 98.9 ± 13.1
White drywall	8.2 ± 0.6; 362.8 ± 35.7	24.0 ± 0.6; 425.5 ± 57.2	2.9 ± 1.2; 62.7 ± 33.3	0.3 ± 0.2; 115.8 ± 10.8
Black drywall	8.4 ± 0.4; 310.8 ± 19.5	24.6 ± 2.5; 493.7 ± 26.7	3.0 ± 1.2; 72.3 ± 48.3	3.5 ± 0.2; 30.9 ± 0.1
Wood	8.5 ± 0.6; 357.8 ± 39.9	26.7 ± 2.5; 496.2 ± 4.4	2.8 ± 1.2; 62.9 ± 34.6	0.3 ± 0.1; 100.2 ± 16.7
Glass	8.6 ± 0.6; 363.5 ± 43.0	26.0 ± 0.4; 371.9 ± 33.2	1.8 ± 1.8; 70.4 ± 51.9	2.6 ± 0.2; 28.2 ± 5.8
Carpet	7.7 ± 0.5; 340.0 ± 35.5	25.6 ± 0.2; 295.4 ± 15.0	0.1 ± 0.03; 63.6 ± 34.4	0.2 ± 0.1; 89.8 ± 16.3
Marble	7.9 ± 1.2; 336.0 ± 11.7	25.4 ± 1.7; 490.0 ± 14.7	3.3 ± 0.9; 92.1 ± 67.2	2.9 ± 0.6; 39.2 ± 1.3
Brick	8.3 ± 0.3; 373.2 ± 45.5	25.6 ± 0.9; 337.4± 47.8	3.5 ± 0.8; 48.8 ± 20.7	1.0 ± 0.1; 61.4 ± 1.9

Table 3: Detection angle across sensors and across obstacle materials.

Material	Polaroid 600	Polaroid 9000	Sharp GP2D02	Sharp GP2D12
Bare drywall	$55.7^0 \pm 4.3^0$	$68.7^0 \pm 3.2^0$	$141.4^0 \pm 10.4^0$	$151.1^0 \pm 1.7^0$
White drywall	$57.2^0 \pm 4.4^0$	$71.7^0 \pm 5.3^0$	$144.1^0 \pm 12.9^0$	$155.0^0 \pm 1.7^0$
Black drywall	$56.6^0 \pm 3.8^0$	$79.4^0 \pm 2.8^0$	$143.9^0 \pm 12.3^0$	$121.2^0 \pm 1.7^0$
Wood	$59.8^0 \pm 3.6^0$	$63.8^0 \pm 2.0^0$	$142.0^0 \pm 10.5^0$	$154.1^0 \pm 1.9^0$
Glass	$54.5^0 \pm 4.4^0$	$55.9^0 \pm 5.6^0$	$124.1^0 \pm 15.1^0$	$72.7^0 \pm 18.8^0$
Carpet	$68.5^0 \pm 6.3^0$	$30.4^0 \pm 4.0^0$	$145.4^0 \pm 10.8^0$	$157.0^0 \pm 2.9^0$
Marble	$68.6^0 \pm 5.1^0$	$95.2^0 \pm 10.7^0$	$135.1^0 \pm 8.2^0$	$128.2^0 \pm 4.5^0$
Brick	$55.3^0 \pm 5.8^0$	$57.3^0 \pm 8.6^0$	$115.7^0 \pm 4.3^0$	$117.3^0 \pm 2.1^0$

Table 4: Detection angle across sensors and across obstacle widths.

Obstacle Width	Polaroid 600	Polaroid 9000	Sharp GP2D02	Sharp GP2D12
1.25 cm	$21.9^0 \pm 4.4^0$	N/A	$18.7^0 \pm 3.6^0$	$15.5^0 \pm 4.0^0$
2.5 cm	$21.6^0 \pm 2.3^0$	$27.6^0 \pm 3.7^0$	$23.9^0 \pm 5.5^0$	$19.1^0 \pm 5.6^0$
5.0 cm	$23.0^0 \pm 2.9^0$	$55.9^0 \pm 4.6^0$	$33.7^0 \pm 3.4^0$	$23.0^0 \pm 2.7^0$
10.0 cm	$47.7^0 \pm 4.7^0$	$68.3^0 \pm 4.1^0$	$48.4^0 \pm 7.2^0$	$43.8^0 \pm 7.6^0$

REFERENCES

1. Fehr L, Langbein W, Skaar S. (2000). Adequacy of Power Wheelchair Control Interfaces for Persons with Severe Disabilities: a Clinical Survey. *Journal of Rehabilitation Research and Development*. 37(3):353-60.
2. Levine S, Bell D, Jaros L, Simpson R, Koren Y, Borenstein J. (1999). The NavChair Assistive Wheelchair Navigation System. *IEEE Trans on Rehab Eng.* 7(4):443-451.

ACKNOWLEDGMENTS

This work was supported by a Phase I SBIR grant from the National Institutes of Health.

Edmund LoPresti
AT Sciences, 5628 Phillips Ave., Pittsburgh, PA 15217
412-901-1042, 412-383-6597 (fax), edlopresti@acm.org

Alternative Text Descriptions

Figure 1: Angle between sensor and obstacle. This figure illustrates the angle between a sensor and an obstacle. Two lines are drawn between a sensor and a flat obstacle. Both lines originate in the center of the sensor. The first line is perpendicular to the obstacle. The second line is perpendicular to the face of the sensor. The angle between these lines, theta, is the angle between the sensor and the obstacle.